Interpreting dynamic soil properties of dry Nevada sand from centrifuge modeling

O.S. Abuhajar, M.H. El Naggar & T. Newson
Geotechnical Research Center, Department of Civil and Environmental Engineering, Western University

ABSTRACT: In seismic analysis, accurate representation of the degradation of the shear modulus and the damping ratio with increasing shear strain levels are considered key features. In this paper, the results of the acceleration time histories obtained at different depths in centrifuge tests, representing free field conditions, were used to investigate the dynamic soil properties of dry Nevada sand. Tests were conducted at two different relative densities (50 and 90%), with two different amplitudes of Western Canada Earthquake. This was done to explore the effect of sand density and shaking acceleration amplitude on the degradation of shear modulus and damping ratio. The effect of different filters was investigated. The results obtained showed that using the unfiltered acceleration to calculate the shear stress and minimum filtered displacement can provide the appropriate shapes for the displacement time history and an acceptable shape for the cyclic loops, as well as reducing the scatter of the damping ratio values.

1 INTRODUCTION

Shear modulus and damping ratios are very important parameters for accurate seismic design. The shear modulus degrades and the damping ratio increases with increase in soil shear strain during earthquake events. Many researchers have previously studied the shear modulus and damping ratio parameters for different soil types under the effect of cyclic loading (e.g. Kokusho, 1980; Rollins et al., 1998; Seed et al., 1986; and Ishibashi & Zhang, 1993). For clean sand, Hardin & Drenvich (1972) found that shear strain, effective stress level, and void ratio are the main factors affecting the shear modulus and damping ratio. Field studies have also been carried out to investigate stiffness nonlinearity based on earthquake motions (e.g. Chang et al. 1989; Zeghal et al. 1995). Zeghal et al. (1995) developed a method to establish the shear modulus and damping ratio from measured acceleration time histories based on evaluating shear stress-strain cycles at different soil depths for instrumented test sites.

Dynamic centrifuge test results can also be used for investigating soil behaviour (Brennan, et al. 2005). The method of Zeghal et al. (1995) has been applied recently to the acceleration time history recorded in centrifuge models (Ellis et al. 1998; Zeghal et al. 1999; Brennan et al. 2005; Elgamal et al. 2005; Rayhani & El Naggar, 2008; Lanzano, et al. 2010).

The research study reported herein investigates the seismic response of dry Nevada sand at two relative densities (50% and 90%), under the effect of the Western Canada Earthquake (WC) with two different amplitudes. The free field acceleration time histories recorded were used to investigate the dynamic soil properties. The effect of acceleration time history filtering was also investigated.

2 CENTRIFUGE MODELING

Two centrifuge tests were performed using the centrifuge at the Rensselaer Polytechnic Institute (RPI), USA, to investigate the seismic response of Nevada sand. The tests involved two different relative densities and seismic loading from the Western Canada earthquake shakings with different amplitudes. The loadings were applied by accelerating the centrifuge from 1g to 60g, and then applying the earthquake shakings at 60g, while continuously monitoring all sensors. The data generated from the acceleration time histories were interpreted to evaluate features of the dynamic soil properties of dry Nevada sand.

2.1 *Nevada sand*

The sand used in the centrifuge tests was 120-Nevada Sand, which is a fine, uniform, and clean sand. Sieve analysis shows that the particle size was in the range of 0.075 to 0.550 mm. This sand is classified as poorly graded sand (SP). The general properties of this sand are shown in Table 1.

2.2 *Earthquake simulation*

The RPI centrifuge facility utilizes a servo-hydraulically controlled system to produce one-dimensional horizontal shaking. This provides input voltage signals and simulates earthquake shakings by applying forces to the model base. The earthquake used was the Western Canada earthquake (shown in Figure 1). Table 2 shows peak ground acceleration (PGA) and the predominant frequency (F_P) of the earthquake input motions. The original earthquake signal was scaled to the desired PGA. Accelerometers were placed in the model to measure the acceleration time history. Each accelerometer was calibrated before installation. The range of accelerations that can be recorded is ± 500g.

2.3 *Model preparation*

The centrifuge container was 876.3 mm (L) × 368.3 mm (W) × 355.6 mm (H). The target sand relative densities for the tests were 50% and 90%. To achieve the required relative densities, the centrifuge box height was divided into layers of 25.4 mm thickness. The sand was placed in the centrifuge box into layers employing air pluviation to achieve the 50% relative density. Each layer was additionally tamped to achieve 90% relative density.

To address the problem of wave reflections due to the rigid sides of the box, an equivalent dummy model was built and subjected to all of the earthquake records with different amplitudes. Several accelerometers were distributed inside the sand at the same elevation and at different distances from the boundary. The recorded acceleration time histories ascertained that there was minimal effect of the boundary on the results and gave essentially the same results. It should be noted that the closest accelerometer to the box side was placed 3 mm from the box side, and that the box wall thicknesses were only 7 mm. Further discussion on the wall boundary conditions are presented elsewhere (Abuhajar, 2013, Abuhajar et al 2015).

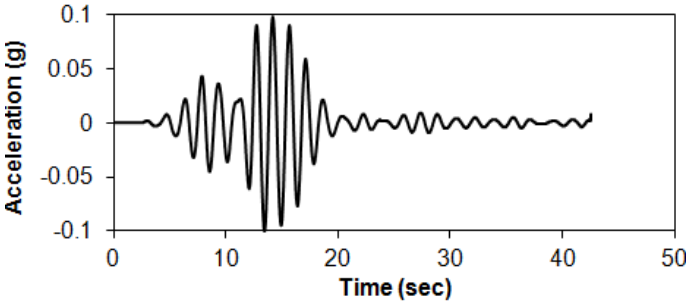

Figure 1. Time history for the Western Canada earthquake.

Table1. General properties of 120-Nevada sand.

Property	Value
Gs	2.67
Effective diameter	D_{10} = 0.080 mm D_{30} = 0.115 mm D_{50} = 0.145 mm D_{60} = 0.160 mm
Uniformity coefficient	C_u = 2.00
Curvature coefficient	C_c = 8.98
Maximum void ratio e_{max}	0.764
Minimum void ratio e_{min}	0.562
Maximum density ρ_{max}	1709.48 kg/m^3
Minimum density ρ_{min}	1513.76 kg/m^3
*Critical State Friction angle ϕ_{cs}	32^o
*Peak Friction angle ϕ_p	40^o
*Peak Dilation angle ψ_p	8^o
*Poisson's ratio	0.28

*After Arulmoli et al (1992) and Lai, et al (2004).

Table 2. Earthquake input motions.

Test	Input motion	Prototype		Centrifuge (1:60)	
		PGA (g)	F_P (Hz)	PGA (g)	F_P (Hz)
T1[a]	WCL	0.09	0.647	5.4	38.8
	WCM	0.24	0.647	14.5	38.8
T2[a]	WCL	0.10	0.647	5.8	38.8
	WCM	0.23	0.647	13.6	38.8

* WC = Western Canada, L = Low, M = Medium.
*T1 & T2 refer to Test1 and Test 2.
*PGA = Peak ground acceleration, F_P = predominant frequency.

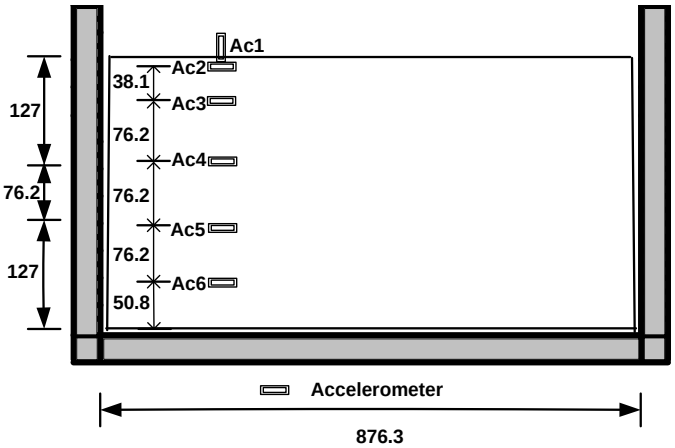

Figure 2. Schematic diagram for centrifuge tests (All units are in mm).

2.4 *Model configuration*

Figure 2 shows the general configurations of the test models. Tests 1 and 2 are for the sand density of 90% and 50 %, respectively. All models were instrumented to measure Free Field acceleration time histories by placing accelerometers inside the sand. As shown in Figure 2, the accelerometers Ac2, Ac3, Ac4, Ac5 and Ac6 were used to measure horizontal acceleration time history along a vertical section. The total height of the sand models was 330 mm, which simulated 19.8 m at 60g. The earthquake signals were sent to the shaker at 60g. Data from all of the sensors were recorded during testing.

3 CENTRIFUGE RESULTS

Data processing and filtering were applied to all acceleration records to remove electronic drift from the records. Filtering is necessary to obtain the correct shape of the velocity and displacement time histories. The data sets chosen for this analysis were from Tests 1 and 2 under the effect of WCL and WCM, to investigate different ranges of shear strain under two relative densities (50% and 90%).

3.1 *Evaluation of shear stress strain history*

The shear stress and shear strain time histories were evaluated using the method proposed by Zeghal et al. (1995). They used a one-dimensional shear beam idealization to describe the site seismic lateral response, assuming 1D vertically propagating shear waves. The shear stress at any level z and time t may be expressed as:

$$\tau_i(t) = \sum_{k=1}^{i-1} \rho \cdot \frac{\ddot{u}_k + \ddot{u}_{k+1}}{2} \cdot \Delta z_k \qquad i = 2, 3, \ldots \qquad (1)$$

where ρ is the mass density in kg/m^3 of the soil, $\ddot{u}$ is the horizontal acceleration and τ is the horizontal shear stress. i refers to level z_i and Δz_k is the spacing interval. The shear stress estimated using Equation 1 is second-order accurate.

The shear strain calculations are based on the displacement time history derived by double integrating the acceleration time history. A second-order accurate shear strain γ_i at level z_i and time t expressed as:

$$\gamma_i(t) = \frac{1}{\Delta z_{i-1} + \Delta z_i}\left[(u_{i+1} - u_i)\frac{\Delta z_{i-1}}{\Delta z_i} + (u_i - u_{i-1})\frac{\Delta z_i}{\Delta z_{i-1}}\right] \qquad (2)$$

where $u_i = u(z_i,t)$ is the absolute displacement.

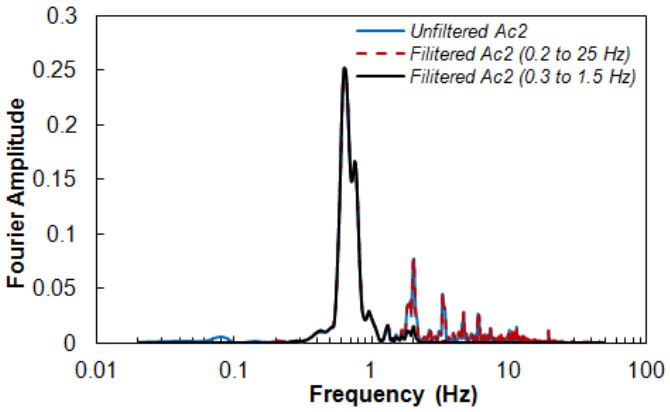

Figure 3. Unfiltered/filtered frequency of acceleration at Ac2

3.2 *Effect of data filtering*

Brennan et al. (2005) recommended filtering the data at high frequency to eliminate noise and at low frequency to eliminate drift errors during integration. The shear stresses and shear strains derived from the acceleration and displacement time histories are very sensitive to the range of filters. The recorded acceleration time histories were first converted to prototype scale and then filtered. The filtering was carried out using the Seismosignal software. This software carries out filtering on the acceleration time history only and the velocity and displacement time histories are the results of the filtered acceleration. The selection of low and high pass filter values was based on the frequency contents of the earthquake signal. Usually, the frequency range in the earthquake signal is between 0 and 25 Hz. Thus, the high pass value was kept at 25 Hz and the low pass value changed until the displacement record had no drift.

A large number of bandpass filters were applied and their effects on the shear stress-strain loops noted. As an example of the unfiltered frequency content of the acceleration time history recorded for the WCL event at Ac2 in Test 1 is shown in Figure 3. To show the effect of filtering on the shear stress-strain loops, two ranges of bandpass filter were applied to this frequency content; one filtered between 0.2 – 25 Hz, and the other between 0.3 – 1.5 Hz, as shown in Figures 3. Using both filter ranges produced an appropriate shape of the displacement time history, but filtering in the 0.3 – 1.5 Hz range can be considered to be heavily over-filtered, because removing the high frequency components removes the details of actual load paths (Brennan et al., 2005).

The shear stress-strain loops were plotted at different depths and there was a clear change in its slope with depth. Due to the limited size of the paper, only the loops from the 16.8 m depth are presented here. The shear stress-strain loops presented in Figures 4 and 5 use filtered and unfiltered accelerations to calculate the shear stresses for the bandpass filter of 0.3 – 1.5 Hz. The results show very

smooth loops when using both filtered acceleration and filtered displacement to get the shear stress and shear strain. This may introduce artefacts because the acceleration time history is over-filtered and causes reduction in the actual values of shear stresses and consequently a reduction in the shear modulus values. Also, the shape of the loops indicates a single frequency record, while earthquakes are multi-frequency records. When using the unfiltered acceleration with the filtered displacement for a bandpass filter of 0.3 – 1.5 Hz, the shape of the loops will be different and will compress and cause the area of the loop to be very small. The damping ratio is a function of the area of the loop, so this may produce small values of damping ratios for such shear strain levels. The shear stress-strain loops for the bandpass filter of 0.2 – 25 Hz is presented in Figures 6 and 7 for filtered and unfiltered accelerations, respectively. The filtered accelerations show very compressed loops, while the unfiltered accelerations produce better shapes for the loops. The authors propose that the unfiltered accelerations will produce more accurate shear modulus, since they use the actual shear stresses and more appropriate shapes for the loops, to achieve more reasonable damping. Therefore, the unfiltered acceleration with the filtered displacement time histories were used to produce the shear stress and shear strain time histories to determine the shear stress-strain hysteresis loops. It is also recommended that the minimum bandpass filter be used that gives the correct shape of displacement time history, since the main purpose is to filter the original acceleration time history records.

3.3 *Calculation of shear modulus & damping ratio*

The procedure for evaluating the shear modulus and damping ratio from shear stress-strain cycle is presented in Figure 8. Each loop was separated to calculate the secant shear modulus and damping ratio. The secant shear modulus G_{sec} calculated as follows:

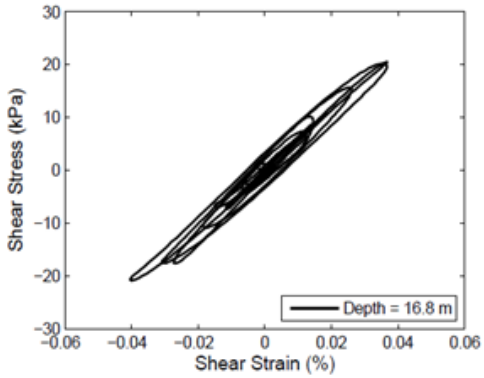

Figure 4. Shear stress-strain cycles at 16.8 m depth during WCL shaking in Test 1 using filtered accelerations and filtered displacements between 0.3 and 1.5 Hz.

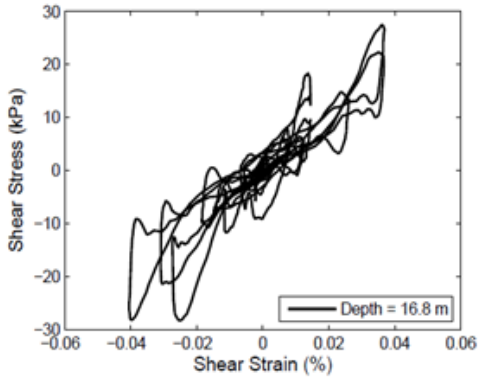

Figure 5. Shear stress-strain cycles at 16.8 m depth during WCL shaking in Test 1 using unfiltered accelerations and filtered displacements between 0.3 and 1.5 Hz.

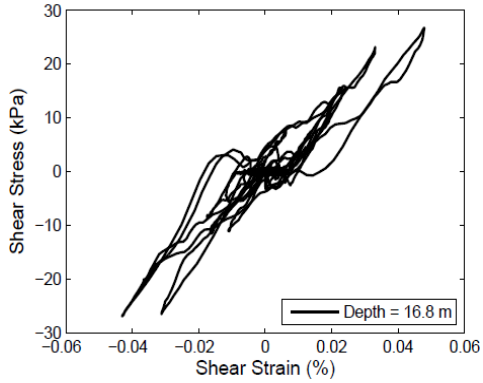

Figure 6. Shear stress-strain cycles at 16.8 m depth during WCL shaking in Test 1 using filtered accelerations and filtered displacements between 0.2 and 25 Hz.

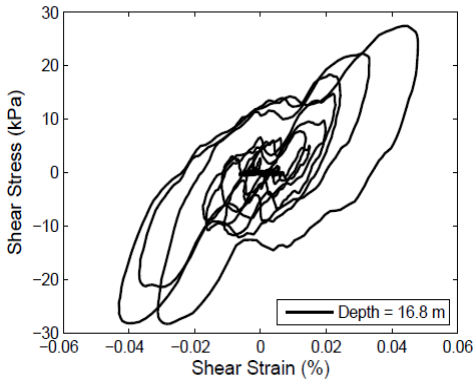

Figure 7. Shear stress-strain cycles at 16.8 m depth during WCL shaking in Test 1 using unfiltered accelerations and filtered displacements between 0.2 and 25 Hz.

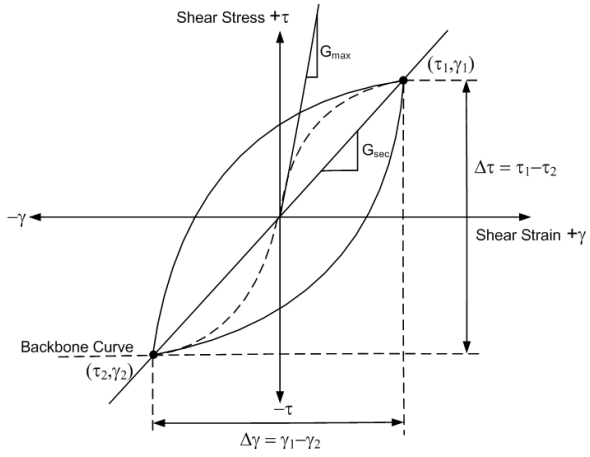

Figure 8. Evaluation of shear modulus and damping ratio from stress-strain loop.

$$G_{sec} = \frac{\Delta\tau}{\Delta\gamma} = \frac{\tau_2 - \tau_1}{\gamma_2 - \gamma_1} \quad (3)$$

where τ_1 and τ_2 are the positive and negative peak shear stresses and γ_1 and γ_2 are the maximum and minimum shear strains, respectively. The damping ratio was calculated using the actual area of loop A_{loop} as shown in the following relation:

$$\xi = \frac{1}{2\pi} \cdot \frac{A_{loop}}{0.25 \times \Delta\tau \times \Delta\gamma} \quad (4)$$

The stress-strain loops were not symmetrical about the shear stress and shear strain axes. In some cases, much of the loop is biased to the positive or negative side of the axes. Therefore, the above procedure is more appropriate than other methods that only use one side of the axis to determine the shear modulus and damping ratio, Abuhajar (2013).

Figure 9 presents a comparison between the filtered and unfiltered accelerations with the filtered displacement for Test 1 using the WCL event. The results show that the filtered accelerations can produce scattered data and cause most of the G/G_{max} and damping ratios to diverge from previous data.

3.4 *Assessment of shear modulus*

Figures 10 and 11 present the results of the normalized secant shear modulus G_{sec} to the maximum shear modulus G_{max} obtained from the backbone curves for Tests 1 and 2 under the earthquake shakings for the WCL and WCM. The results are plotted against the curves given by Seed & Idriss (1970) for a range of dry fine sands. Each point in these Figures represents the result from a single hysteresis loop. The shear strain ranged between 0.005 and 0.2% for Test 1; while for Test 2 it ranged from 0.007 to 0.32%, which is attributed to the difference in sand relative density. It is expected that the less dense sand would experience higher shear strain, especially close to the surface. The effect of the shaking amplitude is clearly shown from the results, since the magnitude of the strain produced by the WCM is larger than that of the WCL. The centrifuge results are in good agreement with the standard curve by Seed & Idriss (1970) and Oztoprak & Bolton (2013).

3.5 *Assessment of damping ratio*

The damping ratios values were estimated from the shear stress-strain loops as a function of the shear strain. Figures 12 and 13 show the results of damping ratio degradation with shear strain for Tests 1 and 2 under the WCL and WCM shakings.

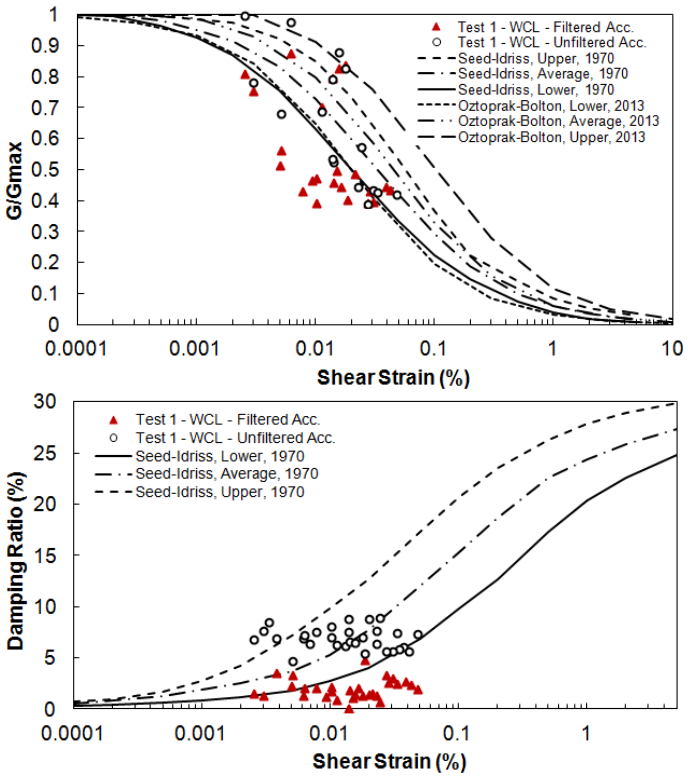

Figure 9. Comparison between the effect of using filtered and unfiltered acceleration with the filtered displacement for Test1.

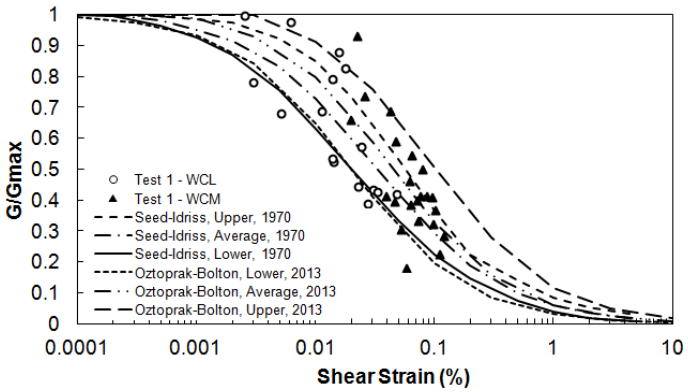

Figure 10. Shear modulus degradation of sand under WCL and WCM shakings in Test 1.

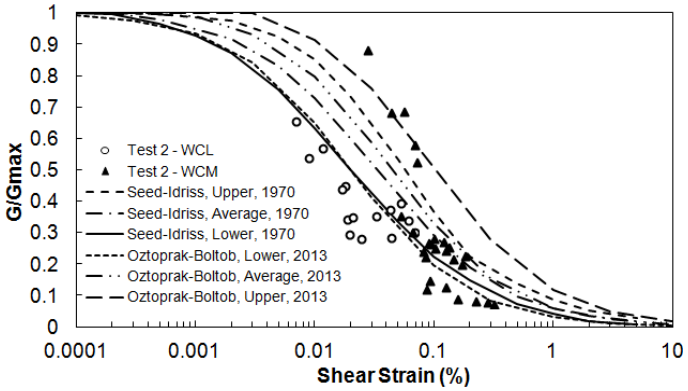

Figure 11. Shear modulus degradation of sand under WCL and WCM shakings in Test 2.

The damping ratios were compared to curves proposed by Seed & Idriss (1970) for dry fine sand and give good agreement. The effect of soil density is also observed in the data. Finally, the adapted filtering procedure resulted in significant reduction in damping scatter similar to Brennan et al. (2005).

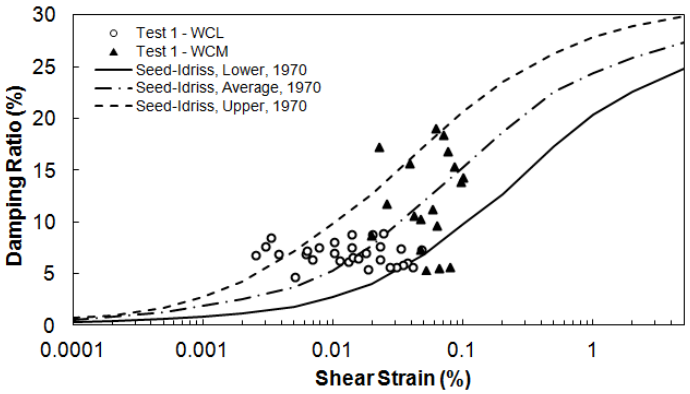

Figure12. Damping degradation of sand under WCL and WCM shakings in Test 1.

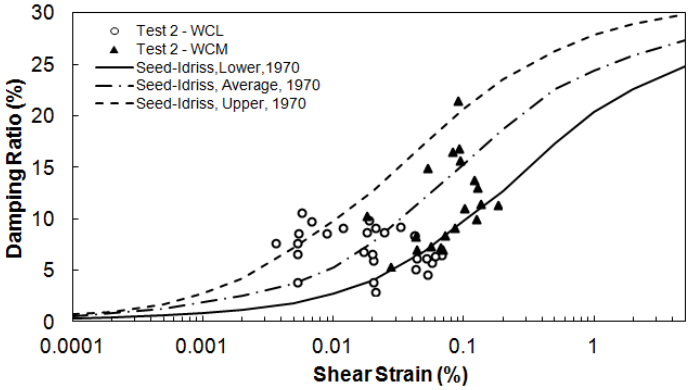

Figure13. Damping degradation of sand under WCL and WCM shakings in Test 2.

4 CONCLUSIONS

Proper evaluation of shear modulus and damping ratio of soil are key factors for accurate seismic analysis. The centrifuge acceleration time histories recorded for free-field locations of the Western Canada earthquake were investigated to examine the shear modulus and damping ratio of the soil and their degradation with shear strain. The effect of filtering of the acceleration time histories on the cycling loops and its effect on the shear modulus and damping ratios were also investigated. Several filtering ranges were examined and it is suggested that the adoption of the minimum filtering range that can produce the appropriate shape of displacement time history is optimal. This shape is recommended to be used to calculate the shear strain time history, while the original (unfiltered) acceleration time history is recommended for use to calculate the shear stress time history. This has the advantage of obtaining the actual shear stress values, with a more reasonable shape of the cyclic loops, and reducing the damping scatter that was observed by other researchers.

5 ACKNOWLEDGEMENT

The authors would like to give thanks to the staff members of the Geotechnical Centrifuge Facility at Rensselaer Polytechnic Institute (RPI) for providing help during this research. The authors would also like to thank NSERC for their financial support.

6 REFERENCES

Abuhajar, O.S., 2013. Static and Seismic Soil Culvert Interaction, PhD dissertation, University of Western Ontario.

Abuhajar, O.S., El Naggar M.H and Newson, T., 2015, Experimental and numerical investigations of the effect of buried box culverts on earthquake excitations, Soil Dynamics and Earthquake Eng J (79): 130 – 148

Arulmoli, K., Muraleetharan, K. K., Hossain, M. M., & Fruth, L. S. 1992. VELACS: Verification of liquefaction analyses by centrifuge studies, laboratory testing program, soil data report. Report - Project No. 90-0562, Irvine, Calif.

Brennan A.J., Thusyanthan N.I., Madabhushi S.P.J. 2005. Evaluation of shear modulus and damping in dynamic centrifuge tests. J of Geotech and Geoenv Eng ASCE 131(12):1488–1497

Chang, C.Y., Power, M.S., Tang, Y.K., & Mok, C.M. 1989. Evidence of nonlinear soil response during a moderate earthquake. *In* Proc 12th Int Conf on Soil Mechanics and Fndt Eng, Balkema, Rotterdam, 1927–1930.

Elgamal, A., Yang, Z., Lai, T., Kutter, B., Wilson, D.W. 2005. Dynamic response of saturated dense sand in laminated centrifuge container. J of Geotech and Geoenv Eng ASCE 131(5):598–609

Ellis, E.A., Soga, K., Bransby, M.F., & Sata, M. 1998. Effect of pore fluid viscosity on the cyclic behavior of sands. *In* Proceedings, Centrifuge 98, T. Kimura, O. Kusakabe, and J. Takemura, eds., Balkema, Rotterdam, 217–222.

Hardin, B.O. & Drnevich, V.P. 1972. Shear modulus and damping in soils: Measurement and parameter effects - Terzaghi Lecture, J of SM & Fndt Eng Div, 98(6):603–624.

Ishibashi, I., & Zhang, X. 1993. Unified dynamic shear moduli and damping ratios of sand and clay. Soils & Fndt, 33(1): 182–191.

Kokusho, T. 1980. Cyclic triaxial test of dynamic soil properties for wide strain range. Soils and Fndts, 20(2): 45–60.

Lai, T., Elgamal, A., Yang, Z., Wilson, D.W., & Kutter, B.L. 2004. Numerical Modeling of Dynamic Centrifuge Experiments on a Saturated Dense Sand Stratum. Proc, 3rd Int Conf on Earthquake Geotechnical Engineering. 1, 558-565.

Luzhen, J., Jun C. & Jie, L. 2010. Seismic response of underground utility tunnels: shaking table testing and FEM analysis. Earthquake Eng and Eng Vibration 9(4): 555-567

Oztoprak, S. & Bolton, M. D. 2013. Stiffness of sands through a laboratory test database Geotechnique 63(1): 54–70

Rayhani, M.H.T., & El Naggar, M.H. 2008. Seismic response of sands in centrifuge tests. Can Geotech J, 45(4): 470–483.

Rollins, K.M., Evans, M.D., Diehl, N.B., & Daily, W.D. 1998. Shear modulus and damping relationships for gravels. J of Geotech and Geoenv Eng, 124(5): 396 - 405.

Seed, H.B., & Idriss, I.M. 1970. Soil moduli and damping factors for dynamic analysis. Rep. No. EERC 70-10, University of California, Berkeley, CA.

Seed, H.B., Wong, R.T., Idriss, I.M., and Tokimatsu, K. 1986. Moduli and damping factors for dynamic analyses of cohesionless soils. J. Geotech. Eng., 112(11): 1016–1032.

Zeghal, M., Elgamal, A.W., Tang, H.T., & Stepp, J.C. 1995. Lotung downhole array. II: Evaluation of soil nonlinear properties. J of Geotech Eng, 121(4): 363 - 378.

Zeghal, M., Elgamal, A.W., Zeng, X., & Arulmoli, K. 1999. Mechanism of liquefaction response in sand-silt dynamic centrifuge tests. Soil Dyn. Earthquake Eng., 18(1): 71 - 85.